Total energy and pressure in the Gaussian-orbitals technique. II. Pressure-induced crystallographic phase transition and equilibrium properties of aluminum

J. C. Boettger and S. B. Trickey
Quantum Theory Project, Department of Physics and Department of Chemistry, University of Florida, Gainesville, Florida 32611
(Received 29 August 1983)

The phase stability of Al as a function of pressure and the bulk properties at equilibrium are explored via a series of all-electron, non—muffin-tin, local-density-functional calculations for the fcc and bcc structures. The techniques used are the linear combination of Gaussian-type orbitals (LCGTO) techniques which we have developed and used to test on bcc Li and fcc Ne recently. The zero-pressure static lattice cohesive energy and lattice constant are in good agreement with experiment, though the computed bulk modulus is less satisfactory. By comparison of the energies and enthalpies of the fcc and bcc structures at various compressions, the fcc phase is found to be more stable for pressures below 3.28 ± 0.09 Mbar with the bcc structure more stable at higher pressure. The current results are compared to previous calculations in an attempt to resolve some major discrepancies between those more approximate calculations (which are both less costly and applicable to a wider variety of crystal structures than present implementations of LCGTO methodology).

I. INTRODUCTION

Calculations, in the local-density-functional (LDF) formalism of the phase stability of elemental crystals as diverse as Xe,[1] rare earth metals,[2] C,[3] Si,[4,5] and third-period metals Al,[5,6] Na, Mg,[5] have been performed with considerable success in recent years. Early work[7] was restricted to modest pressures (few tens of kilobars at most) and was subject to significant numerical limitations,[8] but more recent efforts have explored regimes of quite high pressure with a level of success which is at least qualitative and, frequently, quantitative.

Such calculations are arduous for a number of reasons. In a given crystalline phase, the static-lattice cohesive energy is the difference between the total electronic energy per unit cell of the solid and that of the isolated atom, two numbers which may be as much as six orders of magnitude (as in Xe) and never less than two larger than their difference. Within the assumed local-density model, however, both total energies are variationally stable and if due care is taken to calculate them by procedurally parallel techniques it is quite plausible that a beneficial cancellation of errors (e.g., atomic core energy problems in LDF) will occur. The difference of total energies between crystalline phases is yet smaller, usually by an order of magnitude or more, than the cohesive energy of either phase, so that calculations of the crystalline phase stability can be even more demanding than those of cohesive energy.

The zero-temperature isotherm, of course, does not follow from application of the variational principle to the LDF model, so that transition pressures are even more difficult to calculate than total-energy differences. Further, the zero-temperature isotherm must be calculated in a variety of ways which are identical in principle but may not be when implemented. One such procedure is direct exploitation of the virial theorem (Ry atomic units throughout, except for pressures, which are in kbar):

$$P=(1.47099\times10^5)\left[\frac{E+T}{3N\Omega}\right]. \quad (1)$$

Here T is the total kinetic energy in the assumed local-density model, E the total energy, and N the number of primitive cells each with volume Ω. There is an equivalent surface integral expression which is usually applied in the atomic sphere approximation[9] (ASA). One may also fit the total energy (as a function of volume) to an assumed equation of state and obtain the pressure by differentiation[6] or make a direct approximation of $-dE/dV$ by numerical differences. Whatever the procedure, the fact that E and PV are calculated separately means that the calculated enthalpy $h=E+PV$ will not be a variationally stable quantity though it should be thermodynamically. Since the volume change in passing from one phase to another is often found to be very small, it is not uncommon to compare calculated energy differences, rather than enthalpy differences, on the basis that the resulting imprecision is likely to be lower or at least better controlled in the former procedure.

As might be expected, the severe tasks confronting calculations of crystallographic phase stability have motivated a great variety of approximate techniques not only for obtaining the PV relation but also for obtaining total energies, their differences, etc. Among the more common of these are pseudopotential and linear muffin-tin orbitals[10] (LMTO) procedures. Recent studies of the high-pressure phases of Al have utilized *ab initio* pseudopotentials[6] (AP) and generalized pseudopotential theory[5] (GPT) as well as the LMTO method.[5] Those results agree qualitatively on the sequence of lattices with increasing pressure (fcc→hcp→bcc) but disagree remarkably as to the values of the transition pressures.

We report here a set of LDF calculations on Al employing techniques which rely on an entirely different set of restrictions and approximations from those found in

the LMTO, AP, or GPT techniques. We view these calculations as complementary to those of Refs. 5 and 6. Our methodology is based on the procedure devised by Callaway, Zou, and Bagayoko[11] (CZB) which extends the Callaway-Wang (CW) linear combination of Gaussian-type orbitals (LCGTO) methods[12] to calculation of crystalline total energies. In the preceding paper[13] (hereafter referred to as I) we have shown how to control the CZB methods so that one can calculate a reliable crystalline equation of state directly from the virial theorem.

We summarize pertinent methodological features in Sec. II, present the equation of state and crystal phase stability results in Sec. III, follow in Sec. IV with a discussion of the one-electron results as a function of pressure, and give a brief conclusion in Sec. V.

II. METHODOLOGICAL ASPECTS

LCGTO total energies and virial pressures were computed for six lattice constants in the fcc structure (7.8, 7.6, 7.4, 7.0, 6.4, and 5.6 a.u.) and for four lattice constants in the bcc structure (6.032, 5.556, 5.080, and 4.445 a.u.). At standard pressure and 0 K, the Al lattice constant is reported as 7.60 a.u.[14] The values 7.6, 7.0, 6.4, and 5.6 utilized for the fcc structure calculations correspond to compressions of 1.0, 0.8, 0.6, and 0.4 of the equilibrium volume, while the four lattice constants for bcc produce corresponding cell volumes for that structure. These four volumes are very nearly the same as those used by Lam and Cohen[6] (LC) in their high-pressure study. The two remaining values (in the fcc structure) were selected to allow a decent calculation of the equilibrium lattice constant and bulk modulus B at acceptable computational cost.

Throughout these calculations every attempt has been made to ensure that the input parameters are equivalent with regard to crystal structures for a given molar volume. As in our earlier high-pressure study[13] of Ne, it was necessary to modify the Gaussian basis set as the lattice constant is reduced to avoid linear dependence problems. However, for comparable volumes in the fcc and bcc structures, identical basis sets were used; the five sets required are tabulated in Tables I—V.

TABLE I. The $(12s\,9p\,3d)$ basis set for Al at 7.6 and 7.8 a.u. in the fcc structure as well as for 6.032 a.u. in the bcc structure (see text).

s-type	p-type	d-type
320 000.000 000	259.283 620	5.089 230
54 866.400 000	61.076 870	0.650 000
8 211.766 500	19.303 237	0.169 000
1 866.176 100	7.010 882	
531.129 340	2.873 865	
175.117 970	1.336 596	
64.005 500	0.650 000	
25.292 507	0.341 562	
10.534 910	0.169 000	
3.206 711		
1.152 555		
0.176 678		

TABLE II. The $(12s\,9p\,3d)$ basis set for Al at 7.4 a.u. in the fcc structure (see text).

s-type	p-type	d-type
320 000.000 000	259.283 620	5.089 230
54 866.400 000	61.076 870	0.650 000
8 211.766 500	19.303 237	0.178 259
1 866.176 100	7.010 882	
531.129 340	2.873 865	
175.117 970	1.336 596	
64.005 500	0.650 000	
25.292 507	0.341 562	
10.534 910	0.178 259	
3.206 711		
1.152 555		
0.186 357		

In the fcc calculations the total list of Fourier coefficients was truncated at a maximum value of K^2 (K_M^2; see I) equal to 15 000 [in units of $(2\pi/a)^2$], or 42 956 rotationally independent Fourier coefficients. The corresponding value in the bcc structure is $K_M^2=9500$, or 42 699 independent coefficients. The total number of independent Fourier coefficients allowed to vary from iteration to iteration, N_P (see I), was 80 and 79 in the fcc and bcc structures, respectively.

To achieve a useful analysis of results calculated at only a few molar volumes some form of fitting technique must be employed. In their high-pressure study, LC fitted the four energies they calculated (in each structure) to the Murnaghan[15] equation of state and obtained the pressure by differentiation. For purposes of comparison only, we have applied the Murnaghan equation to our data. The fact that our LCGTO procedure generates both energy and pressure directly at each lattice constant makes a more flexible fitting procedure both possible and useful, however.

We chose a polynomial of the form

$$E(\Omega)/N = E_a + \sum_{i=1}^{4} C_i \Omega^{-\gamma_i} \tag{2}$$

TABLE III. The $(12s\,9p\,3d)$ basis set for Al at 7.0 a.u. in the fcc structure as well as for 5.556 a.u. in the bcc structure (see text).

s-type	p-type	d-type
320 000.000 000	259.283 620	5.089 230
54 866.400 000	61.076 870	0.766 000
8 211.766 500	19.303 237	0.199 000
1 866.176 100	7.010 882	
531.129 340	2.873 865	
175.117 970	1.336 596	
64.005 500	0.766 000	
25.292 507	0.400 000	
10.534 910	0.199 000	
3.206 711		
1.152 555		
0.199 000		

TABLE IV. The (12s 9p 3d) basis set for Al at 6.4 a.u. in the fcc structure as well as for 5.08 a.u. in the bcc structure (see text).

s-type	p-type	d-type
320 000.000 000	259.283 620	5.089 230
54 866.400 000	61.076 870	0.916 601
8 211.766 500	19.303 237	0.238 316
1 866.176 100	7.010 882	
531.129 340	2.873 865	
175.117 970	1.603 198	
64.005 500	0.916 601	
25.292 507	0.481 656	
10.534 910	0.238 316	
3.206 711		
1.152 555		
0.238 316		

TABLE V. The (12s 8p 3d) basis set for Al at 5.6 a.u. in the fcc structure as well as for 4.445 a.u. in the bcc structure (see text).

s-type	p-type	d-type
320 000.000 000	259.283 620	5.089 230
54 866.400 000	61.076 870	0.800 000
8 211.766 500	19.303 237	0.325 412
1 866.176 100	7.010 882	
531.129 340	2.873 865	
175.117 970	1.336 596	
64.005 500	0.650 000	
25.292 507	0.325 412	
10.534 910		
3.206 711		
1.152 555		
0.325 412		

with both the coefficients and exponents determined by fits to the calculated data. In Eq. (2), E_a is set equal to the $X\alpha$ atomic total energy obtained from the Mintmire and Dunlap and Dunlap *et al.* atomic and molecular codes[16] neglecting spin polarization ($E_a = -480.682\,02$ Ry). This choice represents an attempt to reproduce the large volume behavior of $E(\Omega)$ for the paramagnetic crystal (something the Murnaghan equation cannot do), assuming that function to be smooth and attractive at all expanded cell volumes. It must be emphasized that the spin-polarized atomic total energy, $-480.700\,31$ Ry, was used to determine the crystalline cohesive energy. These atomic calculations were executed with the basis set in Table I with one additional s Gaussian (0.065 237) and one additional p Gaussian (0.041 397) added to mimic the effect of off-site orbitals in the crystal.

With E_a determined, a set of exponents γ_i was selected. For any set of exponents, the coefficients C_i were determined uniquely by the requirement that Eq. (2) fit the four energies under consideration (either the four corresponding to lattice points near equilibrium or the four points corresponding to high pressure). The optimum values of the exponents were determined by varying them sequentially to minimize the standard deviation of the pressure derived from Eq. (2) with respect to the calculated pressures.

This procedure has two benefits. It forces the fitting function to match exactly the calculated quantities which are variationally stable in LDF theory, the energies, and it removes the imposition of a prescribed, unalterable volume dependence (such as that given by the Murnaghan equation) upon the calculated data.

III. EQUATION OF STATE AND CRYSTALLINE PHASE STABILITY

The calculated cohesive energies (relative to the spin-polarized atom) and the virial pressures are shown in Table VI for the six primitive cell volumes considered. The primary sources of imprecision in the cohesive energies are the truncation errors in the Fourier sums for E_{xc} and $(U+D)$, and the error introduced by basis-set effects. An estimate of the truncation error in the total energy is obtained by calculating E_{xc} and $(U+D)$ for several values of K_M^2 less than 15 000 (see I); the error in the individual cohesive energies is no more than 0.007 Ry for the three larger volumes, and no more than 0.005 Ry for the three more compressed volumes. Note that these truncation errors are systematic and will always result in cohesive energies which are underestimated (see I).

The major sources of error in the virial pressure are

TABLE VI. The calculated cohesive energies (Ry) and pressures (kbar) for both the fcc and the bcc structures at the six primitive cell volumes Ω (a.u.^{3}) used (see text) and corresponding lattice constants (a.u.).

Ω	a		E_c		P	
	fcc	bcc	fcc	bcc	fcc	bcc
118.6	7.8		−0.2335		−53.9	
109.7	7.6	6.032	−0.2346	−0.2234	−13.3	4.0
101.3	7.4		−0.2308		56.1	
85.8	7.0	5.556	−0.2072	−0.1937	301.1	299.6
65.5	6.4	5.080	−0.1034	−0.0928	1154.1	1103.3
43.9	5.6	4.445	+0.2925	+0.2844	4676.8	4413.7

TABLE VII. Calculated versus fitted pressures (kbar) for Al in the fcc (f) and bcc (b) structures. (M) indicates fitting to the Murnaghan equation while (P) labels the fit from the five-term polynomial in inverse powers of the volume (see text). Each fit is to four values, either high-pressure (h) or low-pressure (l). Standard deviations are given for each fit. The four γ_i for the three polynomial fits above are as follows: $P_l(f)\rightarrow$(1.033 158,2.388 55,4.041 02,7.8654), $P_h(f)\rightarrow$(1.0,2.0,5.0,10.0), and $P_h(b)\rightarrow$(1.0,1.7785,5.0,10.0).

	fcc structure					bcc structure		
Ω (a.u.^{3})	calc. (f)	M_l (f)	P_l (f)	M_h (f)	P_h (f)	calc. (b)	M_g (b)	P_h (b)
118.6	−53.9	−53.5	−48.8					
109.7	−13.3	22.8	20.4	10.9	32.8	4.0	35.5	53.0
101.3	56.1	113.4	117.5					
85.8	301.1	351.2	304.4	386.4	372.0	299.6	387.2	375.7
65.5	1154.1			1284.2	1317.9	1103.3	1232.1	1260.3
43.9	4676.8			5100.1	4677.7	4413.7	4849.4	4417.6
Standard deviation		42.1	35.1	225.8	92.2		231.9	90.6

inadequacies in the core basis set, which primarily affect T, and ordinary numerical imprecision in E [see Eq. (1)]. The former error always should shift the pressure in the negative direction (at least for small Z) since core-basis-set enrichment will increase the core kinetic energy. We found this behavior earlier in both Li and Ne (recall the discussion in I of the effects of a $12s\,8p\,3d$ to $15s\,8p\,3d$ basis change for Ne). By comparison we estimate that basis-set enrichment to saturation (four to six more s-type Gaussians and one to two more p-type) would raise our Al pressures in the vicinity of equilibrium at most 20 kbar. Near equilibrium, an upward shift of the calculated pressures by about 18 kbar would move the predicted zero-pressure lattice constant slightly outside 7.6 a.u., exactly as expected by simple inspection of the calculated cohesive energies alone. These core shifts should be particularly unimportant for structural stability considerations since total energy and pressure differences between phases will largely cancel such shifts.

It is evident from the calculated data that there is a transition from the fcc to the bcc phase between the two more compressed volumes treated. It is also apparent, as noted, that the $X\alpha$ equilibrium lattice constant lies outside the experimental lattice constant, 7.60.[14]

To make more quantitative conclusions, the data must be fitted by an equation of state. The four primitive cell volumes at which both bcc and fcc values were calculated were used to determine the transition point between crystal phases, while the four volumes nearest the experimental zero-pressure volume were fitted to obtain the equilibrium properties. The overall quality of the fit was tested by comparison of the calculated and fitted pressures (see Table VII). We consider the equilibrium and high-pressure properties separately.

A. Equilibrium properties

The polynomial fit, Eq. (2), produced an equilibrium lattice constant of 7.65 a.u. whereas the Murnaghan equation yields 7.66 a.u. Both fits produce a cohesive energy of −0.235 Ry for their respective equilibrium lattice constants. The polynomial fit yields a bulk modulus of 968 kbar as opposed to 1009 kbar from the Murnaghan equation. Even this difference, as large as it is, shows a high consistency between the fits. Since the bulk modulus is determined by the second derivative of $E(\Omega)$, it is reasonable that the values of B determined from the two fits differ somewhat more than do the other calculated quantities. Trial fits to other forms showed the deduced equilibrium properties to be quite insensitive to fitting details. Since the polynomial fit is statistically superior, the results obtained with that fitting technique are compared in Table VIII to several other theoretical calculations[14,17–21] and to experiment.

The experimental static lattice cohesive energy used here (−0.248 Ry/atom) was determined by the usual procedure of subtraction of the zero-point energy of the lattice from the cohesive energy extrapolated to $T=0$ K. The zero-point energy was determined from the zero-temperature Debye temperature, $\Theta_D=423$ K, given by Gschneidner[22] in his Table XV. The zero-temperature cohesive energy is quoted by him (in his Table XII) as −0.245 Ry/atom. Compared to the experimental values, the present $X\alpha$ calculation produces underbinding and a slightly expanded lattice, results that are consistent.

The only other $X\alpha$ results with $\alpha=\frac{2}{3}$ available are those of Ross and Johnson[21] using the augmented plane-wave (APW) method. They obtained a lattice constant somewhat larger than our result. However, they find substantial overbinding where we find slight underbinding. The nonspin-polarized atomic total energy we infer from their paper agrees with the Herman-Skillman value we calculate. They do not say but we suspect that they did not use the spin-polarized atomic total energy. However, that correction is not large enough to eliminate the overbinding that they found. The discrepancy therefore does not appear to arise entirely from the atomic part of the calculations. Given that one would expect the muffin-tin approximation used in the APW method to reduce variational freedom and hence raise the total crystal energy, the cohesive energy from the APW calculation should be smaller in magnitude than that from an LCGTO study using the same LDF model. Such behavior is indeed precisely what we found in Li.[13] There seems, therefore, to

TABLE VIII. The lattice constant (a_e), bulk modulus (B), and the static lattice cohesive energy (E_c) of Al found in this study compared to previous calculations and to experiment.

	a_e (a.u.)	B (kbar)	E_c (Ry/atom)
Chelikowsky (Ref. 17) (Renormalized atom)	8.34	650	−0.219
Lam & Cohen (Ref. 18) (AP)	7.59	715	−0.268
Liberman (Ref. 19) (KKR, Liberman exchange correlation)	7.65	780	−0.245
Janak *et al.* (Ref. 14) (KKR, von Barth-Hedin exchange correlation)	7.59	801	−0.285
Williams *et al.* (Ref. 20) (ASW, von Barth-Hedin exchange correlation)	7.60	870	−0.298
Ross & Johnson (Ref. 21) (APW, $X\alpha$, $\alpha=\frac{2}{3}$)	7.79	940	−0.30
Present calculation (LCGTO, $X\alpha$, $\alpha=\frac{2}{3}$)	7.65	968	−0.235
Experiment (see text)	7.60	794	−0.248

be no obvious explanation for the discrepancy between our results and those of Ross and Johnson.[21]

For the bulk modulus, the experimental value we quote in Table VIII is from the elastic constants reported by Kamm and Alers[23] for $T=4.2$ K. There is extensive disagreement among reported (or attributed) experimental values of the bulk modulus. Anderson (Ref. 24), cited by Janak *et al.*,[14] attributes a $T=0$ K bulk modulus of 880 kbar to de Launay[25] but careful inspection of de Launay's review (especially his Table V) shows that the value 880 kbar actually follows from the 0 K elastic constants of Sutton.[26] Comparison of Sutton's measurements with those of Schmunk and Smith,[27] of Lazarus,[28] of Goen and Weerts,[29] and of Kamm and Alers[23] at room temperature (the only temperature at which the full comparison is available), show that Sutton's values of c_{11} and c_{12} are substantially larger than those found by any other workers. Since $B=(c_{11}+2c_{12})/3$, it is obvious that Sutton's data will predict a larger bulk modulus than that extracted from other worker's results. The consistency of all those other results at room temperature led us to the decision to omit Sutton's data.

We note further that Lam and Cohen[18] quote a room-temperature bulk modulus of 722 kbar from Gschneidner[22] who attributes the value to Bridgman.[30] This latter value seems low relative to the other more recent determinations (which yield a room-temperature value of about 760 kbar). The manifest diversity in the measured values of the bulk modulus of Al, a seemingly simple quantity, is remarkable. It is inappropriate for us as theorists, however, to pursue the issue. In any event, since the bulk modulus of Al falls discernibly with increasing temperature, it seems more suitable to compare 0 K electronic structure calculations with the best available low-temperature experimental value. We believe that to be the value derived from the elastic constant measurements of Kamm and Alers.[23]

B. High-pressure phase stability

Previous studies[5,6] of the phase stability of Al at high pressures have compared the energies (and, in Ref. 6, the enthalpies) for the fcc, hcp, and bcc structures. The CW codes in their present form are restricted to cubic crystals, hence we have only investigated the fcc and bcc structures. This restriction is not a serious drawback since the discrepancies among the earlier work are quantitative not qualitative. In particular, there is significant disagreement between McMahan and Moriarty[5] (MM) and LC as to the transition pressures and volumes but not as to the sequence of phases.

The difference in the static-lattice cohesive energies $[E_c(\text{bcc})-E_c(\text{fcc})]$ obtained in the current investigation is plotted as a function of the relative volume in Fig. 1. [Throughout this discussion the fitting function used is the polynomial of Eq. (2) unless stated otherwise.] The previous *ab initio* self-consistent pseudopotential (AP) (Ref. 6), LMTO (Ref. 5), and GPT (Ref. 5) results are also shown for comparison. For the current LCGTO and the AP results the relative volume scale used is based upon the equilibrium volumes calculated by the two techniques, 112.0 a.u.^{3} and 109.14 a.u.^{3}, respectively. For the LMTO and GPT curves, MM reported the relative volumes with respect to the experimental volume per primitive cell at room temperature and one atmosphere, 112.0 a.u.,^{3} apparently because they did not calculate equilibrium values with either technique.

From Fig. 1 it is clear that our result for the relative volume (and in fact the absolute volume) of the transition from fcc to bcc is in excellent agreement with the AP investigation of LC, and thus disagrees considerably with the transition volumes from the GPT and LMTO work of MM. The transition volume predicted by the present work is 49.97 a.u. Fitting to the Murnaghan equation produced a transition volume of 49.6 a.u., in reasonable

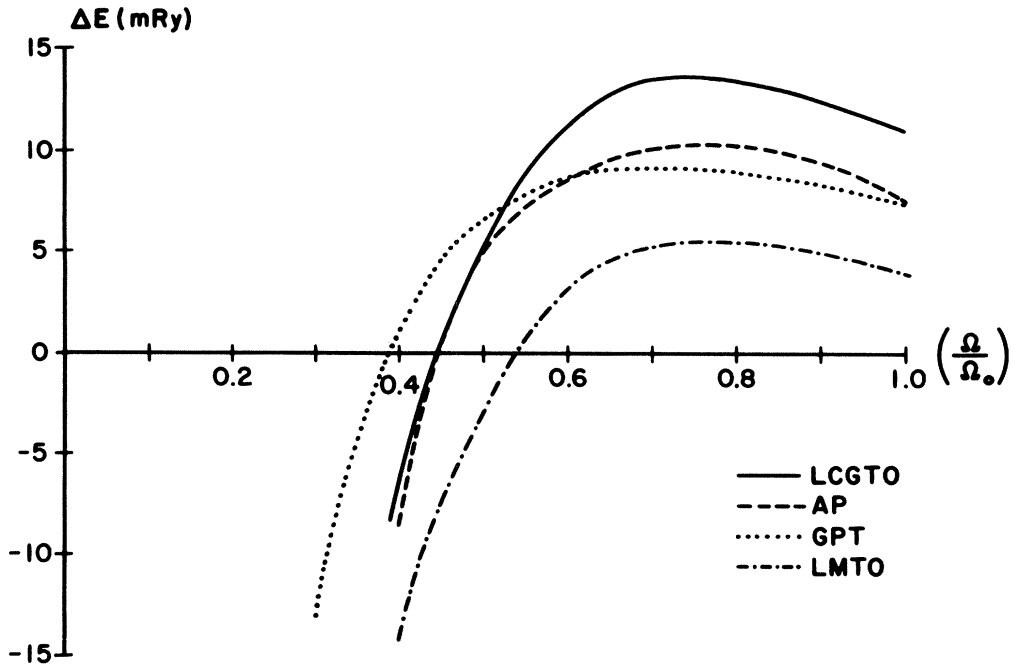

FIG. 1. The difference in energy between the bcc and fcc structures versus volume for the AP (Ref. 6), GPT (Ref. 5), and LMTO (Ref. 5) methods, and the present LCGTO calculation.

agreement with the results from the polynomial fitting procedure shown in Fig. 1, precisely as argued earlier.

It is fitting that the AP prediction of the transition volume agrees best with our result. This conclusion follows from comparison of the substantive approximations made in the two methods. The AP method makes only one such approximation (as opposed to routine matters of numerical procedure) in its solution of the LDF problem, to wit, the use of a frozen core. The LCGTO methodology is, in contrast, an explicitly all-electron technique. It does not make a frozen core approximation. Core relaxation is weakly constrained in the CW version of LCGTO by Fourier-series truncations (see I). Harmon *et al.*[31] studied the frozen core approximation in their LCGTO technique and found all-electron calculations to give perceptibly lower total energies in Si at volume compressions greater than 20%. Such differences should largely cancel between adjacent crystalline phases, precisely the behavior found by LC. Basis-set effects must be controlled carefully in both the LCGTO and AP procedures. Since structural stability is determined by differences in energies calculated with basis sets that are identical except for their crystalline locations, basis-set effects should be inconsequential in both our calculation and that of LC.

In their comparison of accuracy of AP versus LMTO or GPT, MM noted that both the GPT and LMTO utilized substantive approximations beyond those in AP which make both the GPT and LMTO methods "potentially less accurate in structural calculations than the AP method." The extension of that argument to account for the evident differences between our findings and those of MM is straightforward, since the LCGTO procedure is less approximate than the AP method. Of course, the more approximate procedures used by MM enjoy the great advantages of computational speed and applicability to a great variety of crystal structures. In this sense the LCGTO procedure is simply not competitive. However, when the LCGTO method can be used, it clearly has a valuable role as a rigorous implementation of the LDF theory.

At low pressures the LCGTO energy difference is considerably larger than the AP energy difference with the latter approaching the former at compressed volumes. This behavior probably occurs because the exchange-correlation potential used by LC approaches the potential we used in the limit of large densities. The agreement between the LCGTO and AP techniques at high pressures should relieve some of the concern noted by MM about the validity of the AP core treatment at elevated pressures.

Naturally, the transition volume predicted by a comparison of the energies at fixed volumes is only approximate since there will in general be a discontinuity in the volume at the transition. The correct quantity to be studied is the enthalpy ($h=E+PV$) difference. Of the prior calculations only LC studied $h(\Omega)$. In Fig. 2 we compare the enthalpy differences $[h(\text{bcc})-h(\text{fcc})]$ as a function of pressure for the AP and LCGTO techniques. For pressures greater than 1.5 Mbar the two curves are very nearly parallel and are separated by approximately 2 mRy. This is excellent agreement for such small values evaluated as differences between two relatively large quantities.

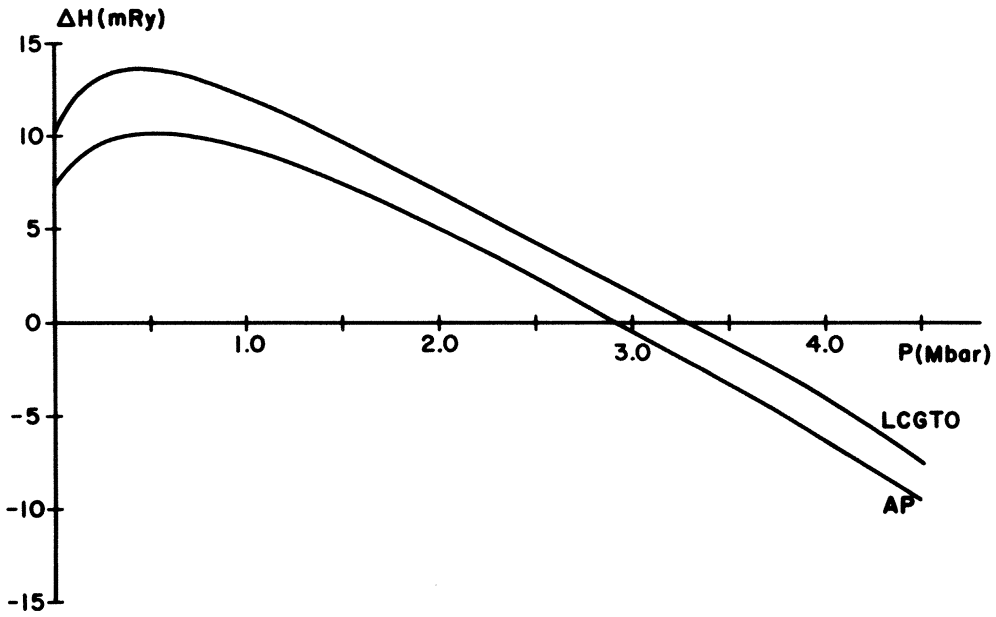

FIG. 2. The difference in enthalpy between the bcc and fcc structures versus pressure for the AP method (Ref. 6) and the present LCGTO calculation.

The LCGTO prediction for the transition pressure is 3.28 ± 0.09 Mbar (the uncertainty here is the standard deviation of the fitting procedure) as opposed to approximately 2.9 Mbar for the AP method. The primitive cell volumes at the fcc-to-bcc phase transition are 50.37 and 49.57 a.u.^{3}, respectively. The volume discontinuity is thus only 0.016 of the fcc volume at the phase transition. The average of the fcc and bcc volumes (49.97 a.u.^{3}) at the calculated transition pressure is exactly the transition volume obtained from the energy. A similar result is found for the pressure discontinuity implied by the fixed volume transition. For this study the implied pressure discontinuity is 0.15 Mbar and the average pressure for the two phases at the transition volume is 3.28 Mbar. These two results are strong confirmation of the assertion by MM that an energy versus volume study (as opposed to enthalpy versus pressure study) of phase stability in Al can be reliable.

IV. ONE-ELECTRON EIGENVALUES

Despite the well-known difficulties with association of the LDF one-electron eigenvalues with physical one-electron excitation energies, it is common to make such an interpretation in metals near the Fermi surface. In this section we adopt that pragmatic view. An important, and certainly less arguable, benefit of studying the one-electron eigenvalues is as a means of comparison of diverse LDF calculations, some of which emphasize the total energy and isotherm while others produce only the one-electron eigenvalues. The sum of those eigenvalues also is used in many total-energy calculations [e.g., Eq. (10) of I]. In fact, MM evaluate structural energy differences (at constant volume) in the LMTO directly from the difference in the sums of the eigenvalues. For these reasons we are obligated to discuss our one-electron results.

For comparison, the most interesting previous energy-band calculation is one by Singhal and Callaway[32] using an earlier version of the CW codes and the same LDF model as we used. Their basis set ($11s\,8p\,5d$) differs from ours ($12s\,9p\,3d$) in ways one might think significant. Our basis set was selected to provide optimum flexibility and fidelity for the representation of the occupied orbitals which, of course, are the critical quantities for a ground-state calculation. This goal must be achieved at a manageable cost. (A five-Gaussian d basis would have resulted in nearly a 40% increase in our computational expenditures.) Since precision is our overriding concern, a test of such d-basis enrichment is required. (One is especially sensitized to this need by the emphasis of both MM and LC on the crucial role that d states play in the high-pressure phase stability of Al, due to hybridization effects near the Fermi level.) Comparison of the Singhal and Callaway band structure with the equilibrium band structure found in this investigation showed no significant differences up through $\Gamma_{25'}$. Since this range extends to energies nearly 1 Ry above the Fermi level, we are confident that our more modest d basis posed no handicap for investigation of ground-state properties, even at highly compressed volumes.

Among the previous high-pressure studies, only MM published an actual band structure at ultrahigh compression ($\Omega/\Omega_0=0.135$). It was for the fcc structure (in spite of the transition to bcc at lower compression) so we restrict this discussion to that phase. Comparison of their high-pressure and normal-pressure band structures reveals several interesting changes. (Their zero-pressure band

structure agrees with ours in all substantive features.) The most important are as follows: (1) The $X_{4'}$ empties and rises above both the X_1 and X_3 states, while the X_3 drops below the Fermi level. (2) The W_3 state moves above the Fermi level while the $W_{2'}$ state drops below, and the W_1 state moves up drastically (out of the figure in MM). (3) The $L_{2'}$ and L_1 states reverse. (4) The K_3 state is driven up through the two K_1 states and the Fermi level.

Direct comparison between our high-pressure band-structure results and those of MM is impaired since the largest compression we considered is 0.4 and MM did not publish results at intermediate pressures. Even so, it is rewarding to study the trends in the fcc Al energy bands under compression. Table IX shows the locations of several points in the energy bands near the Fermi level, relative to the bottom of the conduction band, for compressions of 1.0, 0.8, 0.6, and 0.4 of the experimental volume, 109.74 a.u.^{3} At 0.4 compression we find the following: (1) There is no change at X in the order of the singly degenerate states among themselves or with respect to the Fermi level. In fact, the separation between the $X_{4'}$ and X_3 states has increased by 0.093 Ry (zero-pressure separation equals 0.606 Ry) and the separation between the $X_{4'}$ and X_1 states has only decreased by 0.022 Ry (zero-pressure separation equals 0.098 Ry). (2) At W the reversal in the ordering found by MM (at 0.135 compression) has occurred but the W_3 state is still occupied and lies 0.034 Ry further below the Fermi level, a 52% lowering. (3) At the L point no reversal has occurred and the separation between the L_1 and $L_{2'}$ states has actually increased from 0.017 to 0.176 Ry. (4) At the K point the K_3 state has moved above one of the K_1 states but not the other, and the higher of the K_1 states has moved above the Fermi level.

It might appear that our results disagree significantly with those of MM, but that is not necessarily the case. MM found that the bulk of the change in the LMTO band structure for fcc Al occurred after the lattice reached 0.5 compression (our study only achieved 0.4). The predominant cause of those changes is significant lowering of the energy for the d states relative to both the s and p states. We observed similar lowering of the d states. The disagreement in the trends may be understood at least qualitatively in terms of the relative shift in the s-, p-, and d-type states under pressure.

Inspection of self-consistent Gaussian orbital coefficients for states near the Fermi surface reveals two general trends in the energies of those states as the crystal is compressed. The s states are shifted upward relative to the p states and the d states are shifted down. At zero pressure the singly degenerate states at X, L, and K are ordered with the p states lowest in energy, followed by the s states, then the d states. Initially, compression of the lattice moves the s states up relative to the p states; thus the X_1, L_1, and the higher K_1 states move up relative to the other states near the Fermi level. The trends in our results up to about 0.6 compression are primarily a result of this behavior. Further compression (to 0.4) causes a discernible increase in the d-type character of those same states. Eventually they must drop relative to any states which remain p-type, leading to the reversals in order observed by MM. This trend is foreshadowed clearly by the behavior of the energy difference between the states at X_1 and $X_{4'}$. That difference evidently is largest somewhere between 0.8 and 0.6 compression and decreases with further compression. The ordering of those two states almost certainly must switch for some compression beyond the range investigated here.

The greatest disparity between the trends exhibited in Table IX and the results of MM concerns the separation between L_1 and $L_{2'}$. We find that of all the mixed s- and d-type states the L_1 state has acquired the least d-type character at 0.4 compression and thus any reversal in the shift of L_1 relative to $L_{2'}$ would be expected to occur (if at all) at a higher pressure than does the reversal for the X states.

Although the preceding discussion makes the pressure-induced ordering reversals found by MM quite plausible

TABLE IX. Positions (in Ry) of various points in the fcc Al band structure relative to the bottom of the conduction band, Γ_1 for four compressions relative to the experimental equilibrium volume, 109.744 a.u.^{3} The gaps at X and L ($\Delta X = X_1 - X_{4'}$ and $\Delta L = L_1 - L_2'$) also are given.

Compression	1.0	0.8	0.6	0.4
ϵ_F	0.8205	0.9466	1.0928	1.3312
$X_{4'}$	0.6015	0.6903	0.8051	1.0222
X_1	0.6998	0.8196	0.9418	1.0986
X_3	1.2075	1.3404	1.4924	1.7214
ΔX (gap)	0.0983	0.1293	0.1367	0.0764
W_3	0.7545	0.8637	0.9982	1.2308
$W_{2'}$	0.8294	0.9254	1.0330	1.1925
W_1	0.9067	1.1560	1.4724	2.0314
$L_{2'}$	0.4776	0.5347	0.6066	0.7421
L_1	0.4946	0.5998	0.7228	0.9182
ΔL (gap)	0.0170	0.0651	0.1162	0.1761
K_3	0.6776	0.7765	0.9010	1.1258
K_1	0.7167	0.8093	0.9141	1.0759
K_1	0.7912	0.9579	1.1454	1.4234

our results indicate strongly that those reversals occur at rather higher pressure than found in their LMTO calculation. It is unlikely that differences in the order of levels at high density occur because of detailed differences in the LDF model utilized. The faster pressure-induced lowering of d-type states found in the LMTO calculations of MM (relative to the LCGTO findings) therefore seems likely to be an artifact of the approximations used in the LMTO method. Since the lowering of the d states with pressure appears to be the principal mechanism driving the fcc-bcc transition, one would expect the LMTO prediction of a transition pressure to be lowered with respect to the corresponding LCGTO value. This outcome is especially likely in the case of the LMTO calculations by MM since they evaluated structural energy differences directly from the one-electron eigenvalues.

V. CONCLUSIONS

We have demonstrated that high-precision phase stability studies, including direct-pressure calculations, are both feasible and useful within the CW version of the LCGTO formalism using the modified CZB technique. It is an all-electron, non—muffin-tin methodology which is the most rigorous implementation of LDF theory applied to the Al phase stability problem to date. However, the state of the art for LCGTO calculations is such that there are many systems for which some more approximate, less costly method may be essential. There are at least three techniques (LMTO, GPT, and AP) available from which good qualitative results for the sequence of structural phase transitions with pressure have been obtained for Al. Of those three, we have found the AP method to give the best quantitative agreement with our all-electron calculation of the fcc→bcc transition pressure and volume in Al. In comparison, the LMTO calculation produces a significantly larger transition volume than either the AP or LCGTO calculations, a result which may be due to a too rapid lowering of the d states relative to the p states and the s states in the vicinity of the Fermi level. However, the LMTO method has the distinct advantage of being both fast and relatively simple to apply to unusual crystal structures.

Compared with experiment, our low-pressure results behave in a way consistent with weak underbinding. The $X\alpha$ prediction of the lattice constant at zero pressure is expanded slightly compared to experiment (7.65 versus 7.60 a.u.) while the predicted binding is about 10% too small (-0.235 versus -0.248 Ry). The calculated bulk modulus at equilibrium (968 kbar) can be compared with our best assessment of the experimental value of 794 kbar. At high pressures the bcc structure is more stable than the fcc structure for pressures greater than 3.28 ± 0.09 Mbar. At this transition the average volume is 50.0 a.u.^{3} and the volume discontinuity at the transition is 0.8 a.u.^{3}

ACKNOWLEDGMENTS

We thank the Northeast Regional Data Center of the State University System of Florida for partial support of the computational costs of this study. This work also was supported in part under National Science Foundation Grant No. DMR-82-18498.

[1]M. Ross and A. K. McMahan, Phys. Rev. B 21, 1658 (1980); A. K. Ray, S. B. Trickey R. S. Weidman, and A. B. Kunz, Phys. Rev. Lett. 45, 933 (1980); A. K. Ray, S. B. Trickey, and A. B. Kunz, Solid State Commun. 41, 351 (1982).
[2]H. L. Skriver, Phys. Rev. Lett. 49, 1768 (1982).
[3]M. T. Yin and M. L. Cohen, Phys. Rev. B 24, 6121 (1981).
[4]M. T. Yin and M. L. Cohen, Phys. Rev. Lett. 45, 1004 (1980).
[5]A. K. McMahan and J. A. Moriarty, Phys. Rev. B 27, 3235 (1983); see also, J. A. Moriarty and A. K. McMahan, Phys. Rev. Lett. 48, 809 (1982).
[6]P. K. Lam and M. L. Cohen, Phys. Rev. B 27, 5986 (1983).
[7]F. W. Averill, Phys. Rev. B 4, 3315 (1971).
[8]A. K. McMahan, Phys. Rev. B 17, 1521 (1978).
[9]D. G. Pettifor, Commun. Phys. 1, 141 (1976).
[10]A. R. Mackintosh and O. K. Anderson, in *Electrons at the Fermi Surface,* edited by M. Springford (Cambridge University Press, New York, 1980) and references therein; A. K. McMahan, M. T. Yin, and M. L. Cohen, Phys. Rev. B 24, 7210 (1981).
[11]J. Callaway, X. Zou, and D. Bagayoko, Phys. Rev. B 27, 631 (1983).
[12]C. S. Wang and J. Callaway, Comput. Phys. Commun. 14, 327 (1978).
[13]J. C. Boettger and S. B. Trickey, Phys. Rev. B 29, 6425 (1984); preceding paper.
[14]J. F. Janak, V. L. Moruzzi, and A. R. Williams, Phys. Rev. B 12, 1257 (1975), and references therein.
[15]F. D. Murnaghan, Proc. Natl. Acad. Sci. U. S. A. 30, 244 (1944); O. L. Anderson, J. Phys. Chem. Solids 27, 547 (1966).
[16]J. W. Mintmire and B. I. Dunlap, Phys. Rev. A 25, 88 (1982); see also, B. I. Dunlap, J. W. D. Connolly, and J. R. Sabin, J. Chem. Phys. 71, 3396 (1979).
[17]J. R. Chelikowsky, Phys. Rev. B 21, 3074 (1980).
[18]P. K. Lam and M. L. Cohen, Phys. Rev. B 24, 4224 (1981).
[19]D. A. Liberman, Phys. Rev. B 2, 244 (1970).
[20]A. R. Williams, J. Kubler, and C. D. Gelatt Jr., Phys. Rev. B 19, 6094 (1979).
[21]M. Ross and K. W. Johnson, Phys. Rev. B 2, 4709 (1970).
[22]K. A. Gschneidner, Solid State Phys. 16, 276 (1964).
[23]G. N. Kamm and G. A. Alers, J. Appl. Phys. 35, 327 (1964).
[24]O. L. Anderson, in *Physical Acoustics,* edited by W. P. Mason (Academic, New York, 1965), Vol. III B, Appendix II.
[25]J. de Launay, Solid State Phys. 2, 219 (1956).
[26]P. M. Sutton, Phys. Rev. 91, 816 (1953).
[27]R. E. Schmunk and C. S. Smith, J. Phys. Chem. Solids 9, 100 (1959).
[28]D. Lazarus, Phys. Rev. 76, 545 (1949).
[29]E. Goens and J. Weerts, Phys. Z. 37, 321 (1936).
[30]P. W. Bridgman, Daedalus (Boston) 77, 187 (1949).
[31]B. N. Harmon, W. Weber, and D. R. Hamann, Phys. Rev. B 25, 1109 (1982).
[32]S. P. Singhal and J. Callaway, Phys. Rev. B 16, 1744 (1977); see also, R. A. Tawil and S. P. Singhal, *ibid.* 11, 699 (1975).